

We are IntechOpen, the world's leading publisher of Open Access books Built by scientists, for scientists

6,900

Open access books available

186,000

International authors and editors

200M

Downloads

Our authors are among the

154

Countries delivered to

TOP 1%

most cited scientists

12.2%

Contributors from top 500 universities



WEB OF SCIENCE™

Selection of our books indexed in the Book Citation Index
in Web of Science™ Core Collection (BKCI)

Interested in publishing with us?
Contact book.department@intechopen.com

Numbers displayed above are based on latest data collected.
For more information visit www.intechopen.com



Structural Insight of the Anticancer Properties of Doxazosin on Overexpressing EGFR/HER2 Cell Lines

Martiniano Bello and Miguel Ángel Vargas Mejía

Abstract

The selective α 1-adrenergic receptor antagonist doxazosin is used for the treatment of hypertension. More recently, an experimental report demonstrated that this compound exhibits antiproliferative activity in breast cancer cell lines with similar inhibitory activity to gefitinib, a selective inhibitor of EGFR in the active state (EGFR_{AC}). This experimental study provided evidence that doxazosin can be employed as an anticancer compound, however, the structural basis for its inhibitory properties is poorly understood at the atomic level. To gain insight about this molecule, molecular dynamics (MD) simulation with the molecular mechanics generalized Born surface area (MMGBSA) approach was employed to explore the structural and energetic features that guide the inhibitory properties of doxazosin and gefitinib in overexpressing EGFR/HER2 cell lines. Our result suggest that doxazosin exerts its inhibitory properties in breast cancer cell lines by targeting EGFR/HER2 but mainly HER2 in the inactive state (HER2_{IN}), whereas gefitinib by targeting mainly EGFR_{AC}, in line with previous literature. Decomposition of the binding affinity into individual contributions of HER2_{IN}-doxazosin and EGFR_{AC}-gefitinib systems detected hot spot residues but also showed polar interactions of Met801/Met793 with the quinazoline ring of both compounds. Principal component (PC) analysis revealed that the molecular recognition of the HER2_{IN}-doxazosin system was linked to conformational changes but EGFR_{AC}-gefitinib was not.

Keywords: HER2, EGFR, doxazosin, docking, MD simulations

1. Introduction

Human epidermal growth factor receptor 1 (EGFR) and 2 (HER2) form part of a family of human epidermal grown factor receptors (EGFRs), and whose phosphorylation impacts cell proliferation, differentiation, and migration [1]. The cytoplasmic tyrosine kinase domain (TKD) is considered one of the most studied receptors for developing new anticancer drugs [2]. Activation of EGFR starts the molecular recognition of endogenous growth factors at the extracellular domain that, at the time, promotes the formation of homo- and heterodimers among the different members of EGFR, with HER2 the preferred member of EGFRs to form heterodimers [3–5]. The transition from a monomeric to dimeric state in EGFR is coupled to a conformational change in the TKD from an inactive to active state [6–8], whereas that for

HER2 transitions from inactive, intermediate, and inactive states [9–11]. Generally, the signaling activity regulated by EGFR/HER2 is under control, however, mutations in TKD give place to constitutive activation of these receptors, which results in the development of different types of cancer, such as lung [12] and breast cancer [13]. In addition, overexpression of EGFR/HER2 also happens with radiotherapy and chemotherapy resistance [14–16].

Based on the ability of tyrosine kinase inhibitors (TKIs) to inhibit EGFR, they can be divided in two types, those targeting the active state, such as Iressa, and those targeting the inactive state, such as erlotinib and lapatinib [17–20]. Lapatinib showed dual activity on EGFR/HER2 [21–26]. Despite the benefits of using these TKIs, the employment of them has been linked to severe side effects and drug resistance [27–30]. Therefore, it is necessary to identify new compounds, either through drug design or drug repurposing, that target EGFR and/or HER2 receptors and are effective for cancer therapy. In this context, the combination of docking and molecular dynamics (MD) simulations has been widely exploited to generate new information about the binding properties between natural or synthetic TKIs and EGFR/HER2 [10, 11, 19, 20, 31–36]. In a previous study, Hui et al. explored the inhibitory properties of doxazosin, an α -1 antagonist used for the treatment of hypertension, in two human breast cancer cell lines: BCC MDA-MB-231 and MCF-7 cells [37]. MDA-MB-231 and MCF-7 cells are estrogen receptor (ER) positive and ER negative, respectively [38], and both cell lines also expressed EGFR and HER2; however, MDA-MB-231 expressed both receptors in higher concentrations than MCF-7 [39]. Although EGFR and HER2 are important regulators for normal cellular processes, their dysregulation has been associated to protein overexpression that leads to the development of different types of cancer [1, 5]. They demonstrated that doxazosin induces apoptosis in breast cancer cell lines similar to Iressa (Gefitinib), reducing phosphorylated EGFR by a mechanism that does not involve the α 1-adrenergic receptor, however, the structural and energetic basis for its inhibitory properties is poorly understood. In addition, Sharkawi et al. identified similar experimental antiproliferative activity of doxazosin in an MCF-7 cell line through the inhibition of EGFR [40]. Thus, more robust structural and energetic studies are required to provide structural insight into the affinity of doxazosin for EGFR/HER2 compared with gefitinib. Structural data, docking, and molecular dynamics (MD) simulations combined with the MMGBSA approach were used to elucidate the molecular mechanism through which doxazosin and gefitinib inhibit EGFR/HER2.

2. Methods

2.1 Structural modeling

The free forms of EGFR in the inactive (EGFR_{IN}) and active (EGFR_{AC}) states were taken from the crystallographic structures of EGFR_{IN} (PDB entry 1XKK) and EGFR_{AC} (PDB entry 1M17) conformations. The free forms of HER2 in the inactive (HER2_{IN}) and active (HER2_{AC}) states were taken from previous MD simulation studies; HER2_{IN} [10] and HER2_{AC} [11] conformations. Amino acid residues missing in the electron density map of EGFR structures were built with MODELER Version 9.14 [41].

2.2 Docking studies

Docking calculations were carried out using AutoDock 4.2 and AutoDock Tools 1.5.6 software [42]. The ligand structures were built and optimized with the Gaussian package [43]. The initial geometries of ligands were optimized at the AM1 level. Hydrogen atoms were added to ligands and receptors, and

Kollman and Gasteiger partial charges were assigned for ligand and proteins, respectively. The affinity grid maps were constructed on the receptor using a grid size of $70 \times 70 \times 70 \text{ \AA}$ and 0.370 \AA of spacing. Due to the stochastic nature of the Lamarckian algorithm, 20 runs were performed for each compound, and 30 conformations of the ligand (binding poses) were observed between ligand and protein. The best binding poses were selected using the criteria of having the lowest energetic conformations at the receptor binding site.

2.3 Molecular dynamics simulations

The protein-ligand results obtained by docking were checked through MD simulation studies. MD simulations were carried out using the AMBER16 package [44], in conjunction with the ff14SB force field [45]. The systems simulated were put into a space-filling dodecahedral box of 12 \AA , solvated with TIP3P water model [46], and neutralized with sodium and chloride ions (0.10 M) to create a physiological concentration. The parameterizations of the ligands were performed assigning AM1-BCC atomic charges and matching the atoms with the general Amber force field (GAFF) [47]. Once the systems were constructed, they were minimized using steepest descent with position restraint of the ligands, followed by steepest descent without position restraint and conjugate gradients. The minimized systems were then submitted to 100 ns-long MD simulations using an NPT ensemble with the velocity rescaling arrangement to simulate a constant temperature at 310 K. A constant temperature and pressure (1 atm) were maintained using the weak-coupling algorithm [48], with coupling constants τ_T and τ_P of 1.0 and 0.2 ps, respectively. The electrostatic term was described by the PME method [49], and a 10 \AA cut-off was selected for the van der Waals interactions. The time step for the MD simulations was set to 2.0 fs. The SHAKE algorithm [50] was employed to reset bonds to their right lengths after an unconstrained update. The conformations obtained from MD simulations at intervals of 20 picoseconds (ps) were analyzed using the cptraj tool in Amber16. Plots of variation of root mean squared deviation (RMSD) and radius of gyration (R_G) were generated to evaluate convergence. Clustering analysis using a cutoff of 2.5 \AA was performed to identify the most populated conformation in the simulation. Principal components (PC) analysis along the most essential eigenvectors was carried out to evaluate total flexibility. A map of interactions was generated using Maestro Version 10.1, 2015–1 [51].

2.4 Affinity prediction and per-residue decomposition

The binding free energy (ΔG_{bind}) and per residue contribution were determined using the MMGBSA method [52–55]. Analysis was carried out using a total of 500 protein-ligand conformers at intervals of 100 ps (over the last 50 ns of simulation), considering a salt concentration of 0.10 M and implicit solvent models [56]. The binding free energy (ΔG_{bind}) and per-residue decomposition for each complex was calculated as previously described [11] and were the average result of triplicate experiments.

3. Results and discussion

3.1 Convergence and equilibrium

The stability of the evaluated systems was observed by measuring two geometrical parameters. The root mean squared deviation (RMSD) and the radius of gyration (RG) were determined to identify the time at which the systems reached

3.2 Structural analysis of complexes between doxazosin and EGFR_{AC}/EGFR_{IN}

To explore the structural differences between doxazosin and gefitinib on EGFR/HER2, the most populated receptor-ligand conformations were retrieved over the equilibrated simulation time (the last 50 ns) through clustering analysis. Analysis of the complex between doxazosin and EGFR_{AC} showed that the ligand was stabilized through van der Waals interactions with Phe723, Val726, Leu792, Met793, Pro794, Phe795, Cys797, Leu799, and Leu844, and polar interactions with Gly719, Lys745, Gly796, Asp800, Asp837, Arg841, Asn842, and Asp855 (**Figure 1A**). In contrast, Val718 formed both van der Waals interactions and a hydrogen bond with the quinazoline ring of doxazosin. In the complex with EGFR_{IN}, doxazosin was bound through van der Waals interactions with Phe723, Val718, Val726, Ala743, Leu792, Phe795, Tyr801, and Leu844. The polar contact took place with Lys745, Gln791, Gly796, Glu804, and His805. Met793 formed both van der Waals interactions and one hydrogen bond with the benzodioxin moiety of doxazosin. Pro794 established both van der Waals contacts and one hydrogen bond with the quinazoline ring of doxazosin, whereas Glu804 formed hydrogen bonds with the quinazoline ring of doxazosin (**Figure 1B**). Stabilization of doxazosin did not establish interactions with Thr790 and Met766, two residues whose mutations have been linked to EGFR drug resistance [57, 58]. In addition, the characteristic interactions between Met793 and the quinazoline moiety were not observed, which has previously been observed for other TKIs of EGFR [10].

3.3 Structural analysis of complexes between doxazosin and HER2_{AC}/HER2_{IN}

Doxazosin in complex with HER2_{AC} was bound through van der Waals interactions with Leu726, Val734, Ala751, Phe864, Leu852, and Leu800 and polar interactions with Gly727, Ser783, Thr798, Gln799, Arg849, Thr862, Asp863, and Lys921 (**Figure 1C**). For the complex between doxazosin and HER2_{IN}, the ligand was stabilized by Val754, Leu755, Met774, Leu785, Leu796, Pro802, Cys805, Leu852, and Phe864 and polar contacts with Lys753, Arg756, Gln799, Thr862, and Asp863. Tyr803 and Met801 formed van der Waals and hydrogen bonds with polar groups of the quinazoline ring, whereas Ser783 and Thr798 formed polar contacts with the linker between piperazine and the benzodioxin moiety (**Figure 1D**). Structural comparison of the complexes of doxazosin with HER2_{AC}/HER2_{IN} showed that doxazosin was better coordinated on HER2_{IN} than HER2_{AC} through more well-adjusted types of van der Waals and hydrogen bonds. In addition, the characteristic hinge hydrogen bond between Met801 and the polar atoms of the quinazoline moiety of several TKIs [31, 59] was present only in for the complex with doxazosin and HER2_{IN}.

3.4 Structural analysis of complexes between gefitinib and EGFR_{AC}/EGFR_{IN}

Analysis of complexes between gefitinib and EGFR_{AC} illustrated that the ligand was bound through van der Waals interactions with Leu718, Val726, Ala743, Met766, Leu788, Ile789, Leu792, Pro794, Phe795, Cys797, Leu844, and Phe856. The polar interactions were through contacts with Gly719, Ser720, Gly721, Lys745, Glu762, Thr790, Gln791, Gly796, Arg803, Thr854, and Asp855. Met793 formed van der Waals interactions and one polar interaction with the quinazoline ring of gefitinib, whereas Asp800 formed a hydrogen bond with one of the substituents at the quinazoline ring (**Figure 2A**). In complex with EGFR_{IN}, gefitinib was stabilized by van der Waals contacts with Phe723, Val718, Val726, Ala743, Cys775, Leu792, and

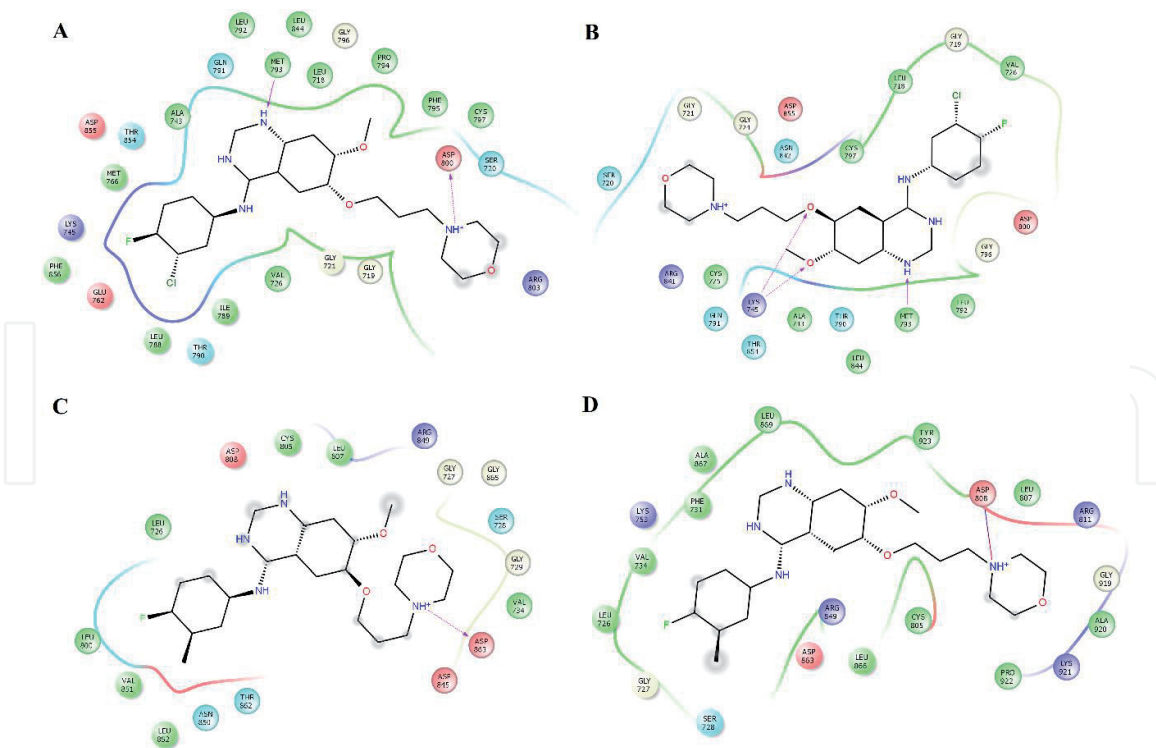


Figure 2.

Map of interactions for the most populated conformation of EGFR/HER2-gefitinib systems. Binding conformations and map of interaction for EGFR_{AC}-gefitinib (A) EGFR_{IN}-gefitinib (B) HER2_{AC}-gefitinib (C) and HER2_{IN}-gefitinib (D). The map of interactions was performed with maestro Schrödinger version 10.1.

Cys797. The polar contacts were through Gly719, Ser720, Gly721, Gly724, Thr790, Gln791, Arg841, Asn842, Thr854, and Asp 855. Met793 established both van der Waals interactions and one hydrogen bond with the quinazoline ring, whereas Lys745 made a hydrogen bond with one of the substituents of the quinazoline ring (**Figure 2B**). Comparison of the map of interactions of both complexes showed that gefitinib was better coordinated on EGFR_{IN} than EGFR_{AC}. In both complexes, gefitinib established interactions with Thr790, a residue whose mutation is linked to EGFR drug resistance [57, 58]. In addition, in both complexes, the characteristic interactions between Met793 and the quinazoline moiety of ligand were observed, which has been reported elsewhere [10].

3.5 Structural analysis of complexes between gefitinib and HER2_{AC}/HER2_{IN}

Gefitinib in complex with HER2_{AC} was bound through van der Waals interactions by Leu726, Val734, Leu800, Cys805, Leu807, Val851, and Leu852 (**Figure 2C**). Polar interactions were stabilized by Gly727, Ser728, Gly729, Asp808, Asp845, Arg849, Asn850, Thr862, and Gly865 residues, whereas Asp863 formed a hydrogen bond with one of the substituents of the quinazoline ring (**Figure 2C**). Gefitinib formed a complex with HER2_{IN}, coordinated by Leu726, Val734, Val731, Cys805, Leu807, Leu866, Ala867, Leu869, Tyr923, Ala920, and Pro922 residues through van der Waals interactions. Polar interactions took place by Gly727, Ser728, Lys753, Arg811, Arg849, Asp863, and Lys921 residues, whereas Asp808 formed a hydrogen bond with one of the quinazoline ring substituents (**Figure 2D**). Structural comparison of both systems depicted that gefitinib was better stabilized on HER2_{IN} than HER2_{AC}. In addition, in both complexes, the characteristic polar interaction between Met801 and polar atoms of the quinazoline moiety of ligand was not observed [31, 59], as observed for the complex between doxasozin and HER2_{IN} (**Figure 1C**).

3.6 Binding free energy

Determination of the ΔG_{bind} values was performed using the MMGBSA method. **Table 2** shows that all systems exhibited thermodynamically favorable ΔG_{bind} values. Nonpolar contributions formed by van der Waals energy (ΔE_{vdw}) and nonpolar desolvation ($\Delta G_{\text{npol,sol}}$) guided the binding of the complexes. Comparative analyses of the complexes between doxazosin or gefitinib on HER2_{AC}, HER2_{IN}, EGFR_{AC}, and EGFR_{IN} showed that doxazosin reached more favorable ΔG_{bind} values on HER2_{IN} than on EGFR_{AC}, EGFR_{IN}, and HER2_{AC}. Gefitinib showed a higher affinity for EGFR_{IN} than EGFR_{AC}, HER2_{AC}, and HER_{IN}. Comparative analysis between the affinity of doxazosin and gefitinib for the four systems showed that doxazosin reached more favorable affinity for HER2_{IN} than gefitinib, whereas gefitinib reached higher affinity for EGFR_{AC} than doxazosin. The results suggested that the inhibitory activity of doxazosin in breast cancer cell lines is by mainly targeting HER2_{IN}, whereas that for gefitinib is mainly through inhibiting EGFR_{AC}, in line with previous studies where the selectivity of gefitinib toward EGFR_{AC} was observed [60]. In addition, this analysis showed that the binding properties of doxazosin could be improved by exploring how changes in the binding affinity of new derivatives of doxazosin coupled on HER2_{IN}.

3.7 Decomposition of the per-residue free energy

This analysis identified the residues that contributed the most to the ΔG_{bind} value for each complex. **Table 3** shows that Leu718, Gly719, Phe723, Val726, Cys797, Leu799, Arg841, and Leu844 were the major contributors in the stabilization of the EGFR_{AC}-doxazosin complex, from which Leu718 established hydrogen bonds with polar atoms of the quinazoline ring of doxazosin (**Figure 1A**). In the EGFR_{IN}-doxazosin complex, Leu718, Val726, Ala743, Leu792, Met793, Pro794, Phe795, Gly796, Tyr801, Glu804, and Leu844 were the main stabilizers of this system. From these residues, Met793, Pro794, and Glu804 formed hydrogen bonds, stabilizing the quinazoline and benzodioxine rings of doxazosin (**Figure 1B**). In the EGFR_{AC}-gefitinib complex, Leu718, Val726, Ala743, Lys745, Met766, Ile789, Thr790, Gln791, Leu792, Met793, Gly796, Cys797, and Thr854 were key residues in the affinity of gefitinib. Among these residues, the participation of Met793 through a hydrogen bond was appreciated (**Figure 2A**), whereas Leu718, Gly719, Val726, Ala743, Lys745, Leu792, Met793, Cys797, Asn842, Leu844, and Thr854 were the major contributors to the ΔG_{bind} value in the EGFR_{IN}-gefitinib complex. Of these residues, the participation of Lys745

Systems	ΔE_{vdw}	ΔE_{ele}	$\Delta G_{\text{ele,sol}}$	$\Delta G_{\text{npol,sol}}$	ΔG_{bind}
EGFR _{AC} -doxazosin	-43.52 (5.13)	22.33 (4.91)	-2.69 (0.80)	-5.46 (0.50)	-29.33 (6.14)
EGFR _{IN} -doxazosin	-38.78 (3.90)	3.25 (0.91)	9.68 (2.80)	-4.62 (0.37)	-30.46 (4.20)
HER2 _{AC} -doxazosin	-36.77 (6.0)	40.15 (12.0)	-21.06 (11.0)	-4.36 (0.55)	-22.05 (4.60)
HER2 _{IN} -doxazosin	-48.93 (4.0)	23.99 (9.0)	-7.39 (1.50)	-5.99 (0.30)	-38.32 (4.0)
EGFR _{AC} -gefitinib	-55.01 (0.16)	-11.11 (0.65)	-25.40 (0.60)	-7.16 (0.01)	-47.88 (0.17)
EGFR _{IN} -gefitinib	-44.10 (0.15)	27.00 (0.69)	-16.48 (0.65)	-5.74 (0.01)	-39.32 (0.23)
HER2 _{AC} -gefitinib	-34.76 (4.0)	38.46 (16.0)	-22.98 (5.0)	-4.90 (0.70)	-24.18 (5.0)
HER2 _{IN} -gefitinib	-38.78 (5.7)	-31.92 (13.0)	49.70 (1.50)	-4.90 (0.50)	-25.91 (6.0)

Table 2.
 Binding free energy components of protein-ligand systems (in units of kcal/Mol).

Residue	EGFR _{AC} -doxazosin	EGFR _{IN} -doxazosin	EGFR _{AC} -gefitinib	EGFR _{IN} -gefitinib
Leu718	-1.071	-2.243	-1.664	-1.261
Gly719	-0.532			-0.871
Phe723	-2.805			
Val726	-1.325	-0.674	-2.183	-1.705
Ala743		-0.548	-1.188	-0.592
Lys745			-0.782	-2.276
Met766			-0.727	
Ile789			-0.520	
Thr790			-1.190	
Gln791			-0.186	
Leu792		-1.257	-1.663	-1.897
Met793		-1.394	-2.045	-1.618
Pro794		-0.696		
Phe795		-2.053		
Gly796		-1.43	-1.122	
Cys797	-1.622		-1.015	-1.109
Leu799	-0.672			
Tyr801		-0.737		
Glu804		-1.064		
Arg841	-1.904			
Asn842				-0.504
Leu844	-0.935	-0.809		-2.063
Thr854			-0.839	-1.069

Table 3.

Per-residue free energy for complexes between doxazosin and gefitinib with EGFR_{AC}/EGFR_{IN} (values kcal/Mol).

and Met793 were important in the stabilization of quinazoline and substitution at the quinazoline ring (**Figure 2B**).

Table 4 shows that Leu726, Gly727, Ser728, Val734, Asp863, and Phe864 contributed the most to the ΔG_{bind} value of the HER2_{AC}-doxazosin complex. Met774, Ser783, Leu785, Leu796, Thr798, Met801, Tyr803, Gly804, Cys805, Leu852, Thr862, and Phe864 were the major residues stabilizing the HER2_{IN}-doxazosin complex. The participation of Ser783, Thr798, Met801, and Tyr803 was visualized through the formation of hydrogen bonds with gefitinib (**Figure 1D**). Leu726, Cys805, Leu807, Arg849, Asn850, Leu852, and Thr862 were the main contributors in the HER2_{AC}-gefitinib complex (**Table 4**). Leu726, Phe731, Val734, Cys805, Leu807, Arg849, Leu866, Pro922, and Tyr923 contributed the most to the ΔG_{bind} value in the HER2_{IN}-gefitinib complex.

3.8 Principal component analysis

We evaluated the differences in mobility for the free and bound EGFR/HER2 systems via PC analysis. Evaluation of the quantification of the diagonalized covariance matrix based on covariance showed the following values: HER2_{AC}, 15.0 nm²;

Residue	HER2 _{AC} -doxazosin	HER2 _{IN} -doxazosin	HER2 _{AC} -gefitinib	HER2 _{IN} -gefitinib
Leu726	-1.913		-0.67	-0.551
Gly727	-1.056			
Ser728	-0.756			
Phe731				-2.184
Val734	-1.163			-0.855
Met774		-0.56		
Ser783		-0.837		
Leu785		-1.414		
Leu796		-1.069		
Thr798		-1.122		
Met801		-2.045		
Tyr803		-1.854		
Gly804		-0.652		
Cys805		-1.1	-1.378	-0.531
Leu807			-0.844	-0.597
Arg849			-2.104	-2.011
Asn850			-0.559	
Leu852		-2.069	-1.026	
Thr862		-2.25	-0.757	
Asp863	-1.631			
Phe864	-0.828	-1.09		
Leu866				-0.822
Pro922				-1.358
Tyr923				-1.685

Table 4.
 Per-residue free energy for complexes between doxazosin and gefitinib with HER2_{AC}/HER2_{IN} (values kcal/Mol).

HER2_{AC}-doxazosin, 10.26 nm²; HER2_{AC}-gefitinib, 8.83 nm²; HER2_{IN}, 28.9 nm²; HER2_{IN}-doxazosin, 18.21 nm²; HER2_{IN}-gefitinib, 20.41 nm²; EGFR_{AC}, 10.79 nm²; EGFR_{AC}-doxazosin, 9.46 nm²; EGFR_{AC}-gefitinib, 7.69 nm²; EGFR_{IN}, 8.17 nm²; EGFR_{IN}-doxazosin, 11.55 nm²; and EGFR_{AC}-gefitinib, 10.0 nm². This result indicates that the molecular recognition of doxazosin or gefitinib on HER2_{AC}, HER2_{IN}, and EGFR_{AC} decreased the number of conformational states compared to that of free HER2_{AC}, HER2_{IN}, and EGFR_{AC} states. However, this conformational reduction was more significant for the free and bound HER2_{IN} system. In contrast, a small increase in the conformational mobility was experienced upon the coupling of gefitinib by EGFR_{IN}. This indicated that doxazosin and gefitinib binding to HER2_{IN} was linked with reduced heterogeneity, which suggests that this molecular recognition was associated with an unfavorable entropy contribution that could contribute to decrease the favorable ΔG_{bind} values for HER2_{IN}-doxazosin and HER2_{IN}-gefitinib, as seen in **Table 2**.

4. Conclusion

In this chapter, we explored the structural and energetic features that guide the similar inhibitory properties of doxazosin with gefitinib in overexpressing

EGFR/HER2 cell lines combining docking and MD simulation with the MMGBSA approach. Based on these studies, we identified that doxazosin was able to target the active and inactive states of EGFR and HER2, however, its inhibitory activity against breast cancer cell lines was mainly by targeting HER2_{IN}. Similarly, although gefitinib was able to target the inactive and inactive states of EGFR and HER2, its activity mainly targeted EGFR_{AC}, in line with previous reports. Per-residue free energy analysis identified the key residues stabilizing HER2_{IN-DOX} and EGFR_{AC-GEF} systems, showing that in the stabilization of both systems, Met793 and Met801 were involved for EGFR and HER2, respectively. These residues stabilized HER2_{IN-DOX} and EGFR_{AC-GEF} systems through the formation of hydrogen bonds with the quinazoline ring, as reported for other TKIs. This study provides structural and energetic information that can be used to design new inhibitors for HER2_{IN} or EGFR_{AC} using doxazosin or gefitinib, respectively, as a pharmacophoric model.

Acknowledgements

This is an unpublished original article. The work was supported by grants from CONACYT (CB-A1-S-21278) and SIP/IPN (20201015).

Author details

Martiniano Bello^{1*} and Miguel Ángel Vargas Mejía²

¹ Laboratorio de Diseño y Desarrollo de Nuevos Fármacos e Innovación Biotecnológica de la Escuela Superior de Medicina, Instituto Politécnico Nacional, México

² Departamento de Biomedicina Molecular, Centro de Investigación y de Estudios Avanzados del Instituto Politécnico Nacional (CINVESTAV-IPN), Ciudad de México, México

*Address all correspondence to: bellomartini@gmail.com and mbellor@ipn.mx

IntechOpen

© 2021 The Author(s). Licensee IntechOpen. This chapter is distributed under the terms of the Creative Commons Attribution License (<http://creativecommons.org/licenses/by/3.0>), which permits unrestricted use, distribution, and reproduction in any medium, provided the original work is properly cited. 

References

- [1] M.A. Olayioye, R.M. Neve, H.A. Lane, N.E. Hynes, The ErbB signaling network: receptor heterodimerization in development and cancer, *EMBO J.* 19 (2000) 3159-3167.
- [2] G. Lurje, H.-J. Lenz, EGFR signaling and drug discovery, *Oncology* 77 (6) (2009) 400-410.
- [3] E. Tzahar, H. Waterman, X. Chen, G. Levkowitz, D. Karunakaran, S. Lavi, B.J. Ratzkin, Y. Yarden. A hierarchical network of interreceptor interactions determines signal transduction by Neu differentiation factor/neuregulin and epidermal growth factor. *Mol. Cell. Biol.* 16 (1996), pp. 5276-5287
- [4] X. Qian, C.M. LeVea, J.K., Freeman, W. C. Dougall, M.I. Greene. Heterodimerization of epidermal growth factor receptor and wild-type or kinase-deficient Neu: a mechanism of interreceptor kinase activation and transphosphorylation. *Proc. Natl. Acad. Sci. U. S. A.*, 91 (1994), pp. 1500-1504
- [5] D. Graus-Porta, R.R. Beerli, J. M. Daly, N.E. Hynes. ErbB-2, the preferred heterodimerization partner of all ErbB receptors, is a mediator of lateral signaling. *EMBO J.*, 16 (1997), pp. 1647-1655
- [6] D.J. Riese 2nd, R.M. Gallo, J. Settleman, Mutational activation of ErbB family receptor tyrosine kinases: insights into mechanisms of signal transduction and tumorigenesis, *BioEssays* 29 (2007) 558-565.
- [7] X. Zhang, J. Gureasko, K. Shen, P.A. Cole, J. Kuriyan, An allosteric mechanism for activation of the kinase domain of epidermal growth factor receptor, *Cell* 125 (2006) 1137-1149.
- [8] S.R. Hubbard, W.T. Miller, Receptor tyrosine kinases: mechanisms of activation and signaling, *Curr. Opin. Cell Biol.* 19 (2007) 117-123.
- [9] K. Aertgeerts, R. Skene, J. Yano, B.-C. Sang, H. Zou, G. Snell, A. Jennings, K. Iwamoto, N. Habuka, A. Hirokawa, T. Ishikawa, T. Tanaka, H. Miki, Y. Ohta, S. 15 Sogabe. Structural analysis of the mechanism of inhibition and allosteric activation of the kinase domain of HER2 protein. *J. Biol. Chem.*, 286 (2011), pp. 18756-18765
- [10] Bello, M., Guadarrama-García, C. & Rodriguez-Fonseca, R.A. Dissecting the Molecular Recognition of Dual Lapatinib Derivatives for EGFR/HER2. *J Comput Aided Mol Des* 2020 Mar; 34(3):293-303.
- [11] Bello, Martiniano, et al. "Structural and energetic basis for the molecular recognition of dual synthetic vs. natural inhibitors of EGFR/HER2." *International journal of biological macromolecules* 111 (2018): 569-586.
- [12] S.V. Sharma, D.W. Bell, J. Settleman, D.A. Haber, Epidermal growth factor receptor mutations in lung cancer, *Nat. Rev. Cancer* 7 (2007) 169-181.
- [13] J.R.C. Sainsbury, J.R. Farndon, G.K. Needham, A.J. Malcolm, A.L. Harris, Epidermal growth-factor receptor status as predictor of early recurrence of and death from breast-cancer, *Lancet* 1 (1987) 1398-1402
- [14] F. Ciardiello, G. Tortora. A novel approach in the treatment of cancer: targeting the epidermal growth factor receptor. *Clin Cancer Res.*, 7(2001), pp. 2958-2970
- [15] B.N. Rexer, R. Ghosh, A. Narasanna. Human breast cancer cells harboring a gatekeeper T798M mutation in HER2 overexpress EGFR ligands and are sensitive to dual inhibition of EGFR and HER2. *Clin Cancer Res.*, 19(2013), pp. 5390-401
- [16] I.M. Gonzaga, S.C. Soares-Lima, P.T. de Santos. Alterations in epidermal

growth factor receptors 1 and 2 in esophageal squamous cell carcinomas. *BMC Cancer*, 12(2012), pp. 56

[17] E.R. Wood, A.T. Truesdale, O.B. McDonald, D. Yuan, A. Hassell, S.H. Dickerson, B. Ellis, C. Pennisi, E. Horne, K. Lackey, K.J. Alligood, D.W. Rusnak, T.M. Gilmer, L. Shewchuk. A unique structure for epidermal growth factor receptor bound to GW572016 (Lapatinib): relationships among protein conformation, inhibitor off-rate, and receptor activity in tumor cells. *Cancer Res.*, 64 (2004), pp. 6652-6659

[18] M.A. Seeliger, P. Ranjitkar, C. Kasap, Y. Shan, D.E. Shaw, N.P. Shah, J. Kuriyan, D.J. Maly. Equally potent inhibition of c-Src and Abl by compounds that recognize inactive kinase conformations. *Cancer Res.*, 69 (2009), pp. 2384-2392

[19] M. Bello. Binding mechanism of kinase inhibitors to EGFR and T790M, L858R and L858R/T790M mutants through structural and energetic analysis. *International journal of biological macromolecules*, 118 2018, pp. 1948-1962

[20] L. Saldaña-Rivera, M. Bello, D. Méndez-Luna. Structural insight into the binding mechanism of ATP to EGFR and L858R, and T790M and L858R/T790 mutants. *Journal of Biomolecular Structure and Dynamics*, 1 (2019), pp. 1-14

[21] D.W. Rusnak, K. Lackey, K. Affleck. The effects of the novel, reversible epidermal growth factor receptor/ ErbB-2 tyrosine kinase inhibitor, GW2016, on the growth of human normal and tumor-derived cell lines in vitro and in vivo. *Mol. Cancer Ther.*, 1 (2001), pp. 85-9

[22] G.E. Konecny, M.D. Pegram, N. Venkatesan, R. Finn, G. Yang. Activity of the dual kinase inhibitor lapatinib (GW572016) against

HER-2- overexpressing and trastuzumab-treated breast cancer cells. *Cancer Res.*, 66 (2006), pp. 1630-1639

[23] S.R. Johnston, A. Leary. Lapatinib: a novel EGFR/HER2 tyrosine kinase inhibitor for cancer. *Drugs Today Barc*, 42 (2006), pp. 441-453

[24] Y. Zhou, S. Li, Hu YP, J. Wang, J. Hauser. Blockade of EGFR and ErbB2 by the novel dual EGFR and ErbB2 tyrosine kinase inhibitor GW572016 sensitizes human colon carcinoma GEO cells to apoptosis. *Cancer Res.*, 66 (2006), pp. 404-411

[25] P.J. Medina, S. Goodin. Lapatinib: a dual inhibitor of human epidermal growth factor receptor tyrosine kinases. *Clin. Ther.*, 30 (2008), pp. 1426-1447

[26] S.R. Johnston, A. Leary, Lapatinib: a novel EGFR/HER2 tyrosine kinase inhibitor for cancer, *Drugs Today (Barc)* 42 (2006) 441-453.

[27] B. Forsythe, K. Faulkner, Overview of the tolerability of gefitinib (IRESSA) monotherapy: clinical experience in non-small-cell lung cancer, *Drug Saf.* 27 (2004) 1081-1092.

[28] D.M. Jackman, V.A. Miller, L.A. Cioffredi, B.Y. Yeap, P.A. Jänne, G.J. Riely, M.G. Ruiz, G. Giaccone, L.V. Sequist, B.E. Johnson, *Clin. Cancer Res.* 15 (2009) 5267.

[29] W. Pao, V.A. Miller, K.A. Politi, G.J. Riely, R. Somwar, M.F. Zakowski, M.G. Kris, H. Varmus, Acquired resistance of lung adenocarcinomas to gefitinib or erlotinib is associated with a second mutation in the EGFR kinase domain, *PLoS Med.* 2 (2005), e73.

[30] C.H. Yun, K.E. Mengwasser, A.V. Toms, M.S. Woo, H. Greulich, K.K. Wong, M. Meyerson, M.J. Eck, The T790M mutation in EGFR kinase causes drug resistance by increasing the affinity for ATP, *PNAS* 105 (2008) 2070-2075.

- [31] M. Ahmed, M. Sadek, K. A. Abouzid, F. Wang. In silico design: extended molecular dynamic simulations of a new series of dually acting inhibitors against EGFR and HER2. *Journal of Molecular Graphics and Modelling*, 44 (2013), pp. 220-231
- [32] M.M. Sadek, R.A. Serrya, A.-H.N. Kafafy, M. Ahmed, F. Wang, K.A.M. Abouzid, Discovery of new HER2/EGFR dual kinase inhibitors based on the anilinoquinazoline scaffold as potential anticancer agents, *J. Enzyme Inhib. Med. Chem.* 1 (2013) 1-8.
- [33] S.C. Yang, S.S. Chang, H.Y. Chen, C.Y.C. Chen, Identification of potent EGFR inhibitors from TCM database@ Taiwan, *PLoS Comput. Biol.* 7 (10) (2011), e1002189.
- [34] Y. Liu, N.S. Gray, Rational design of inhibitors that bind to inactive kinase conformations, *Nat. Chem. Biol.* 2 (2006) 358-364.
- [35] C.N. Cavasotto, R.A. Abagyan, Protein flexibility in ligand docking and virtual screening to protein kinases, *J. Mol. Biol.* 337 (2004) 209-226.
- [36] B. Chandrika, J. Subramanian, S.D. Sharma, Managing protein flexibility in docking and its applications, *Drug Discov. Today* 14 (2009) 394-400.
- [37] Hui, Hongxiang, Manory A. Fernando, and Anthony P. Heaney. "The α 1-adrenergic receptor antagonist doxazosin inhibits EGFR and NF- κ B signalling to induce breast cancer cell apoptosis." *European journal of cancer* 44.1 (2008): 160-166.
- [38] Ford, Christopher HJ, et al. "Reassessment of estrogen receptor expression in human breast cancer cell lines." *Anticancer research* 31.2 (2011): 521-527.
- [39] Stanley, Aryan, et al. "Synergistic effects of various Her inhibitors in combination with IGF-1R, C-MET and Src targeting agents in breast cancer cell lines." *Scientific Reports* 7.1 (2017): 1-15.
- [40] El Sharkawi, Fathia Zaky, Hany Abdelaziz El Shemy, and Hussein Moustafa Khaled. "Possible anticancer activity of rosuvastatine, doxazosin, repaglinide and oxcarbazepin." *Asian Pacific Journal of Cancer Prevention* 15.1 (2014): 199-203.
- [41] A. Sali, T.L. Blundell, Comparative protein modelling by satisfaction of spatial restraints, *J. Mol. Biol.* 234 (3) (1993) 779-815.
- [42] G.M. Morris, R. Huey, W. Lindstrom, M.F. Sanner, R.K. Belew, D.S. Goodsell, A.J. Olson, *Computational Chemistry* 16 (2009) 2785-2791.
- [43] M.J. Frisch, G.W. Trucks, H.B. Schlegel, G.E. Scuseria, M.A. Robb, J.R. Cheeseman, J.A. Montgomery, Jr., T. Vreven, K.N. Kudin, J.C. Burant, J.M. Millam, S.S. Iyengar, J. Tomasi, V. Barone, B. Mennucci, M. Cossi, G. Scalmani, N. Rega, G.A. Petersson, H. Nakatsuji, M. Hada, M. Ehara, K. Toyota, R. Fukuda, J. Hasegawa, M. Ishida, T. Nakajima, Y. Honda, O. Kitao, H. Nakai, M. Klene, X. Li, J.E. Knox, H.P. Hratchian, J.B. Cross, V. Bakken, C. Adamo, J. Jaramillo, R. Gomperts, R.E. Stratmann, O. Yazyev, A.J. Austin, R. Cammi, C. Pomelli, J.W. Ochterski, P.Y. Ayala, K. Morokuma, G.A. Voth, P. Salvador, J.J. Dannenberg, V.G. Zakrzewski, S. Dapprich, A.D. Daniels, M.C. Strain, O. Farkas, D.K. Malick, A.D. Rabuck, K. Raghavachari, J.B. Foresman, J.V. Ortiz, Q. Cui, A.G. Baboul, S. Clifford, J. Cioslowski, B.B. Stefanov, G. Liu, A. Liashenko, P. Piskorz, I. Komaromi, R.L. Martin, D.J. Fox, T. Keith, M.A. Al-Laham, C.Y. Peng, A. Nanayakkara, M. Challacombe, P.M.W. Gill, B. Johnson, W. Chen, M.W. Wong, C. Gonzalez, and J.A. Pople, *Gaussian 03, Revision B.04*, Gaussian, Inc., Wallingford, CT, 2004

- [44] D.A. Case, T.E. Cheatham, T. Darden, H. Gohlke, R. Luo, K.M. Merz Jr., R.J. Woods, The Amber biomolecular simulation programs, *J. Comput. Chem.* 26 (2005) 1668-1688
- [45] Y. Duan, C. Wu, S. Chowdhury, M.C. Lee, G. Xiong, W. Zhang, et al., A point-charge force field for molecular mechanics simulations of proteins based on condensed phase quantum mechanical calculations, *J. Comput. Chem.* 24 (16) (2003) 1999-2012
- [46] W.L. Jorgensen, J. Chandrasekhar, J.D. Madura, R.W. Impey, M.L. Klein, Comparison of simple potential functions for simulating liquid water, *J. Chem. Phys.* 79 (1983) 926-935.
- [47] J. Wang, R.M. Wolf, J.W. Caldwell, P.A. Kollman, D.A. Case, Development and testing of a general amber force field, *J. Comput. Chem.* 25 (9) (2004) 1157-1174
- [48] H.J.C. Berendsen, J.P.M. Postma, W.F. van Gunsteren, A. DiNola, J.R. Haak, Molecular dynamics with coupling to an external bath, *J. Chem. Phys.* 81 (8) (1984) 3684-3690.
- [49] T. Darden, D. York, L. Pedersen, Particle mesh Ewald-an N. log(N) method forwald sums in large systems, *J. Chem. Phys.* 98 (1993) 10089-10092.
- [50] W.F. Van Gunsteren, H.J.C. Berendsen, Algorithms for macromolecular dynamics and constraint dynamics, *Mol. Phys.* 34 (1977) 1311-1327.
- [51] Maestro, version 10.1. Schrödinger, LLC; New York, NY, USA: 2015-1.
- [52] B.R. Miller, T.D. McGee, J.M. Swails, N. Homeyer, H. Gohlke, A.E. Roitberg. MMPBSA.py: an efficient program for end-state free energy calculations. *J. Chem. Theory Comput.*, 8 (2012), pp. 3314-3321
- [53] H. Gohlke, C. Kiel, D. A. J. Case. Insights into protein-protein binding by binding free energy calculation and free energy decomposition for the Ras-Raf and Ras-RalGDS complexes. *Mol. Biol.*, 330 (2003), pp. 891-913
- [54] P.A. Kollman, I. Massova, C. Reyes, B. Kuhn, S. Huo, L. Chong. Calculating structures and free energies of complex molecules: combining molecular mechanics and continuum models. *Acc. Chem. Res.*, 33 (2000), pp. 889-897
- [55] J. M. Wang, T. J. Hou, X. J. Xu. Recent advances in free energy calculations with a combination of molecular mechanics and continuum model. *Drug Des.*, 2 (2006), pp. 287-306
- [56] A. Onufriev, V. Bashford, D. A. Case. Exploring protein native states and large-scale conformational changes with a modified generalized born model. *Proteins.*, 55 (2004), pp. 383-394
- [57] C.H. Yun, K.E. Mengwasser, A.V. Toms, M.S. Woo, H. Greulich, K.K. Wong, M. Meyerson, M.J. Eck. The T790M mutation in EGFR kinase causes drug resistance by increasing the affinity for ATP. *PNAS*, 105 (2008), pp. 2070-2075
- [58] Z. Ruan, S. Katiyar, N. Kannan. Computational and Experimental Characterization of Patient Derived Mutations Reveal an Unusual Mode of Regulatory Spine Assembly and Drug Sensitivity in EGFR Kinase. *Biochemistry*, 56(2017), pp. 22-32
- [59] Xing, L., Klug-Mcleod, J., Rai, B., & Lunney, E. A. (2015). Kinase hinge binding scaffolds and their hydrogen bond patterns. *Bioorganic & medicinal chemistry*, 23(19), 6520-6527.
- [60] J.H. Park, Y. Liu, M.A. Lemmon, R. Radhakrishnan, Erlotinib binds both inactive and active conformations of the EGFR tyrosine kinase domain, *Biochem. J.* 448 (3) (2012) 417-423